

Supporting Information

© Wiley-VCH 2014

69451 Weinheim, Germany

Racemic DNA Crystallography**

*Pradeep K. Mandal, Gavin W. Collie, Brice Kauffmann, and Ivan Huc**

anie_201409014_sm_miscellaneous_information.pdf

Supporting information

1	Materials and methods	S2
1.1	Materials	S2
1.2	Racemic DNA Crystallogensis	S2
1.3	X-ray diffraction	S2
1.4	Structure determination and refinement	S2
1.5	Crystal structure of D/L -TG ₄ T in <i>P</i> -1 space group	S2
1.6	Crystal structures of D/L -G ₄ T ₄ G ₄ in <i>P</i> -1 and <i>P</i> 2 ₁ / <i>n</i> space groups	S3
1.7	Crystal structure of D/L -CCGGTACCGG in <i>C</i> 2/ <i>c</i> space group	S3
1.8	Crystal structures of D/L -CCGGTACCGG in <i>P</i> -1 space group	S4
2	Supplementary Figures	S5
Figure S1:	Comparison of crystal packing of racemic and non-racemic crystal structures of bimolecular G-quadruplexes formed from the sequence d(G ₄ T ₄ G ₄).	S5
Figure S2:	Comparison of crystal packing of racemic and non-racemic crystal structures of B-type duplexes formed from the sequence d(CCGGTACCGG) (bound by cobalt).	S6
Figure S3:	Comparison of crystal packing of racemic and non-racemic crystal structures of four-way DNA junctions formed from the sequence d(CCGGTACCGG).	S7
Figure S4:	Comparison of crystal packing of racemic and non-racemic crystal structures of tetramolecular G-quadruplexes formed from the sequence d(TG ₄ T).	S8
3	Tables	S9
Table S1:	Comparison of racemic and non-racemic DNA crystallogensis.	S9
Table S2:	X-ray diffraction data and refinement statistics	S10
Table S3:	Root mean square deviation (RMSD) values of the reference D-DNA crystal structures superposed to D-DNA structures obtained from racemic crystallization.	S11
Table S4:	Comparison of resolution and solvent content of racemate with the reference D-DNA crystal structures	S12
4	References	S13

1 Materials and methods

1.1 Materials

L- and D- deoxyribonucleic acids were purchased from ChemGenes Corporation (USA) on a 3 μ mole synthesis scale with HPLC purification. These oligonucleotides were used without further purification. Stock solutions were prepared using ultra-pure water to single strand concentrations of 4 mM.

1.2 Racemic DNA Crystallogenesis

Solutions of L- and D- oligodeoxyribonucleotides were separately prepared and mixed in equimolar amounts and incubated for 1 hour at 293 K. Crystallization experiments were set up using the hanging drop vapour diffusion method with siliconized cover slips and Linbro 24-well crystallization plates. The racemic crystallogenesis experiments are detailed in Table S1 and in the subsequent paragraphs.

1.3 X-ray diffraction

For low temperature X-ray diffraction data collection (at 100 K), single crystals were flash frozen in liquid nitrogen. Diffraction data were collected on (i) an *in-house* micro-focus rotating anode Rigaku FRX with Cu K α radiation; (ii) the PROXIMA 1 beam line at Synchrotron SOLEIL and (iii) the ID23-2 Gemini beam line at the European Synchrotron Radiation Facility (ESRF). All diffraction data were processed using the software package XDS (Kabsch, 2010). X-ray diffraction data collection statistics are detailed in Table S2.

1.4 Structure determination and refinement

All structures reported in this work were solved by molecular replacement using the program PHASER (McCoy *et al.*, 2007). The structures were refined using REFMAC5 (Murshudov *et al.*, 2011) from the CCP4 software package (Winn *et al.*, 2011) and *phenix.refine* (Afonine *et al.*, 2012) from the PHENIX suite (Adams *et al.*, 2010). Translation libration screw (TLS) refinement was carried out in the initial round of refinements with the parameters generated in *phenix.refine* (Afonine *et al.*, 2012) using each strand of the asymmetric unit as a separate TLS group. After each refinement step, visual inspection of the model and the electron-density maps were carried out using Coot (Emsley *et al.*, 2010), using both $2F_o - F_c$ and $F_o - F_c$ difference maps. Ions and water molecules were added throughout different stages of refinement as indicated by the electron density in the appropriate $F_o - F_c$ difference maps. The difference Fourier maps were contoured at 5 σ and 3 σ levels in order to place the ions and water molecules respectively. Occupancy refinement was carried out to ensure no negative density at certain positions in subsequent maps. Root mean square deviation values were determined using Superpose (Krissinel and Henrick, 2004) and figures were prepared using the program PyMOL (DeLano, 2002). The coordinates and structure factors have been deposited in the Protein Data Bank (Berman *et al.*, 2000) (accession codes are provided in Table 1). Full refinement statistics are detailed in Table S2.

1.5 Crystal structure of D/L-TG₄T in P-1 space group

The crystallization conditions reported for the crystal structure of the D-TG₄T sequence (Phillips *et al.*, 1997; Caceres *et al.*, 2004; Lee *et al.*, 2007) were initially tried for the racemic D/L-TG₄T mixture (at 277 K), however, no crystals were obtained in these conditions. Sparse-matrix screening was then carried out using a Jena Bioscience Screen kit (JB Screen Basic 1) at 293 K, followed by systematic optimization of one crystallisation condition (described in Table S1). Tiny, rectangular crystals appeared after 30 days and grew to their maximal dimensions within 75 days.

X-ray diffraction data were collected on an *in-house* microfocus rotating anode Rigaku FRX diffractometer, with Cu K α radiation and a hybrid pixel detector (Dectris Pilatus 200K). The data

were limited to a resolution of 2.69 Å (Table S2). The crystal belongs to the *P*-1 space group with unit-cell parameters $a = 39.94$, $b = 39.00$, $c = 84.08$ Å; $\alpha = 103.34^\circ$, $\beta = 103.37^\circ$, $\gamma = 90.04^\circ$. The Matthew's (V_M) coefficient and solvent content for these crystals were 2.02 Å³Da⁻¹ and 59 % respectively, with four molecules in the asymmetric unit (Matthews, 1968).

The structure was determined by molecular replacement using the G-quartet core of a tetramolecular G-quadruplex structure (PDB ID 352D; Phillips *et al.*, 1997) as an initial search model. The best molecular replacement solution indicated the presence of four tetramolecular G-quadruplexes stacked one on top of each other in the asymmetric unit. Visual inspection of the difference Fourier maps and symmetry related molecules indicated (i) a void space in the pseudo-continuous arrangement of the G-quadruplexes and (ii) the absence of any electron density for the terminal thymine nucleotides at the 3' end. A total of 14 K⁺ ions were identified from the difference Fourier ($F_o - F_c$) maps. The final refinement statistics are shown in Table S2. Figure 2d shows the overall structure of the D/L-TG₄T mixture along with K⁺ ions.

1.6 Crystal structures of D/L-G₄T₄G₄ in *P*-1 and *P*2₁/*n* space groups

The crystallization conditions reported for D-G₄T₄G₄ (Haider *et al.*, 2002; Hazel *et al.*, 2006) were initially used in an attempt to crystallise the D/L-G₄T₄G₄ racemic mixture (at 285 K). Two crystal forms (form I and II) were obtained for two very similar growth conditions, differing only in the concentration of MgCl₂ (shown in Table S1). Chunky, colour-less, rod-like crystals appeared after 30 days and grew to their maximum dimensions within 45 and 90 days, for crystal forms II and I, respectively.

X-ray diffraction data were collected *in-house*. The two crystal forms (I and II) were limited to a resolution of 1.90 and 1.85 Å respectively (Table S2). Crystal form I belongs to *P*-1 space group with unit cell parameters $a = 27.65$, $b = 28.30$, $c = 45.72$ Å; $\alpha = 104.50^\circ$, $\beta = 94.19^\circ$, $\gamma = 113.42^\circ$. Crystal form II belongs to the *P*2₁/*n* space group with unit cell parameters $a = 28.50$, $b = 47.30$, $c = 46.80$ Å; $\beta = 97.02^\circ$.

The Matthew's (V_M) coefficients of 2.06 and 2.07 Å³Da⁻¹; and solvent contents of 60% for both crystal forms indicated the presence of one bimolecular G-quadruplex in the asymmetric unit for each crystal form (Matthews, 1968). Molecular replacement was carried out using coordinates of bimolecular G-quadruplexes 2HBN and 1JRN as initial search models, for crystal forms I and II, respectively (Gill *et al.*, 2006; Haider *et al.*, 2002). The best molecular replacement solution for both crystal forms clearly indicated the presence of one bimolecular anti-parallel G-quadruplex in the asymmetric unit. TLS refinement was carried out with each strand as a separate TLS group. The L- and D- bimolecular G-quadruplexes were found to stack one above the other in a pseudo-continuous manner as shown in Supplementary figure 1a. Five K⁺ ions coordinated to the G-quartets were identified in both crystals forms. The final refinement statistics are shown in Table S2.

1.7 Crystal structure of D/L-CCGGTACCGG in *C*2/*c* space group

Bevelled, diamond-shaped crystals of the sequence D/L-CCGGTACCGG were grown in 7 days at 293 K, after optimizing the crystallisation conditions reported for the sequence D-CCGGTACCGG (Eichman *et al.*, 2000) (Table S1). X-ray diffraction data were collected on the Proxima 1 beam line at Synchrotron SOLEIL. The data were limited to a nominal resolution of 2.33 Å (Table S2). The crystal belongs to the monoclinic *C*2/*c* space group, with unit cell dimensions $a = 65.95$, $b = 23.35$, $c = 72.91$ Å; $\beta = 94.19^\circ$.

The Matthew's coefficient (2.09 Å³Da⁻¹) and solvent content (60%) indicated the presence of two DNA strands in the asymmetric unit. The structure was solved by molecular replacement using the D-CCGGTACCGG structure reported as a four-way Holliday junction (PDB ID 1DCW, Eichman *et al.*, 2000) as a search model. The model consisted of a non-crossing strand and a crossing strand (the crystallographic two-fold symmetry axis generates the full junction by a two-

fold rotational symmetry operation). TLS refinement was carried out with the two strands of the asymmetric unit as two separate TLS groups. One Ca^{2+} and one Na^+ ion were identified in the major groove site for the two strands. The final refinement statistics are given in Table S2.

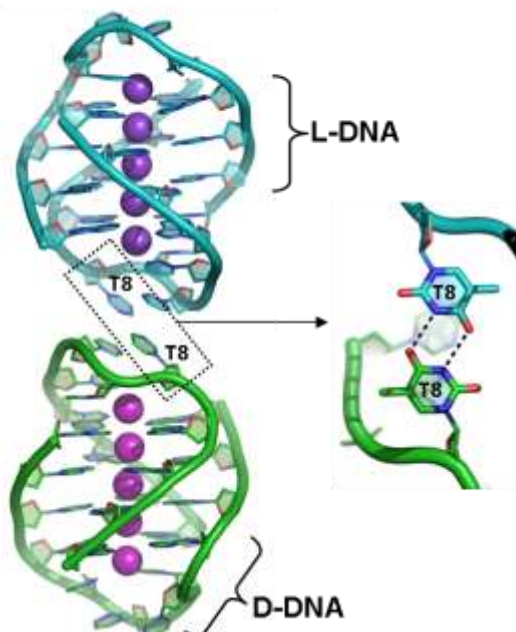
1.8 Crystal structures of D/L-CCGGTACCGG in *P*-1 space group

This sequence was known to be amphimorphic, with the possibility to pack as either a four-way Holliday junction in low salt conditions in the crystallization drop or as a B-type duplex DNA in higher salt conditions in the crystallization drop (Venkadesh *et al.*, 2012). We prepared a crystallization screen for this sequence composed of varying concentrations of sodium cacodylate buffer (pH 7.0), divalent salts such as $\text{CaCl}_2 \cdot 2\text{H}_2\text{O}$, $\text{MgCl}_2 \cdot 6\text{H}_2\text{O}$, and $\text{CoCl}_2 \cdot 6\text{H}_2\text{O}$ and spermine. The crystallization drops were equilibrated against a reservoir solution composed of 20-40 % 2-methyl-2,4-pentanediol (MPD). The optimized conditions are described in Table S1. Chunky, triclinic crystals were obtained for crystallization drops containing either $\text{CaCl}_2 \cdot 2\text{H}_2\text{O}$, $\text{MgCl}_2 \cdot 6\text{H}_2\text{O}$ or $\text{CoCl}_2 \cdot 6\text{H}_2\text{O}$. All three crystal forms diffracted to high resolution (1.28, 1.29, and 1.49 Å respectively) and were all found to belong to the *P*-1 space group. Unit cell parameters for the Ca and Co forms were isomorphous with one another, whereas the cell dimensions of the Mg form were larger (see Table S2). Analyses of the cell contents indicated the presence of two strands in the asymmetric unit for the Ca and Co forms, and four strands in the asymmetric unit for the Mg form (see Table S2).

Structures for each of the three crystal forms were determined by molecular replacement using the B-type duplex DNA reported by Venkadesh *et al.*, 2012 (PDB ID 3R86) as a search model. The overall structure was similar to the B-type DNA double helix, with local structural variations due to the ion interactions and packing arrangements. In each of the structures, we were able to identify the primary cations bound to the DNA atoms. Figure 2 shows the position of the ions around these double helices. All these duplex structures were found to be highly hydrated. The tight packing of the L- and D- duplexes could be the reason for the high resolution of the diffraction data. The final refinement statistics are given in Table S2.

2 Supplementary Figures

a) Racemic structure of D/L d(G₄T₄G₄)
Space group: *P*-1



b) Non-racemic structure of D d(G₄T₄G₄)
Space group: *P*2₁2₁2₁

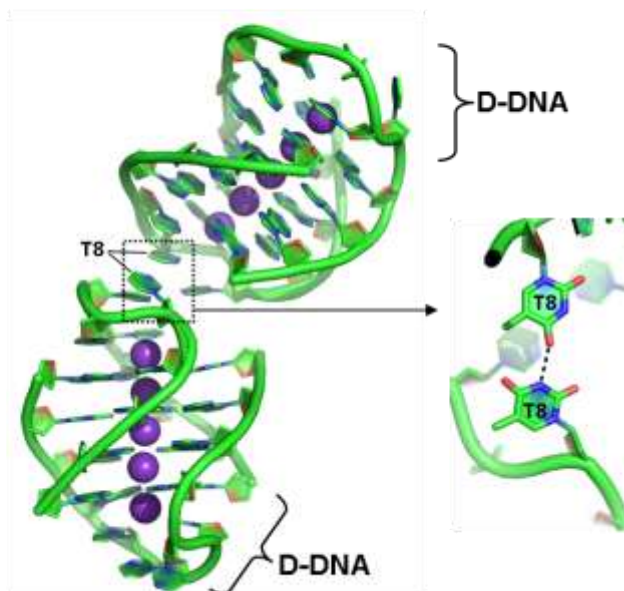
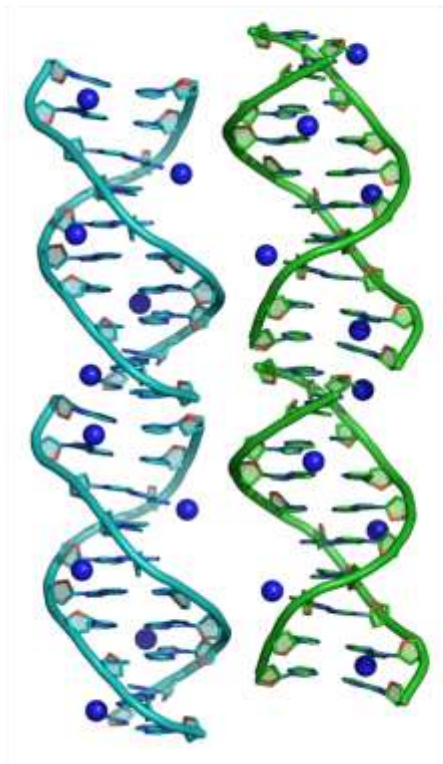


Figure S1: Comparison of crystal packing of racemic and non-racemic crystal structures of bimolecular G-quadruplexes formed from the sequence d(G₄T₄G₄).

a) Racemic crystal structure of D/L-d(G₄T₄G₄) in space group *P*-1. Thymine 8 of the D-enantiomer (green) forms an unusual TT base pair with the equivalent thymine 8 residue of a neighbouring L-enantiomer DNA molecule (cyan), involving mirrored hydrogen bonds between the N3 and O4 groups of the base (bond distances = 2.9 Å). This TT base pair is also seen in the second racemic crystal form determined for this sequence (in space group *P*2₁/*n*). b) Crystal packing of the equivalent D-enantiomer crystal structure (PDB ID: 1JRN, sequence: D-d(G₄T₄G₄) [Haider *et al.*, 2002]). The packing of the D-enantiomers is similar to the racemic mixture in that both crystal forms exploit the thymine ‘loops’ for packing contacts, however, the restricted packing options of the pure D-enantiomer structure results in a TT base pair involving just one hydrogen bond (between the N3 and O4 groups) (bond distance = 2.7 Å). D-DNA, green; L-DNA, cyan; potassium ions, magenta spheres.

a) **Racemic structure of a B-type duplex**
Sequence: D/L d(CCGGTACCGG)
Space group: $P-1$



b) **Non-racemic structure of a B-type duplex**
Sequence: D d(CCGGTACCGG)
Space group: $P6_1$

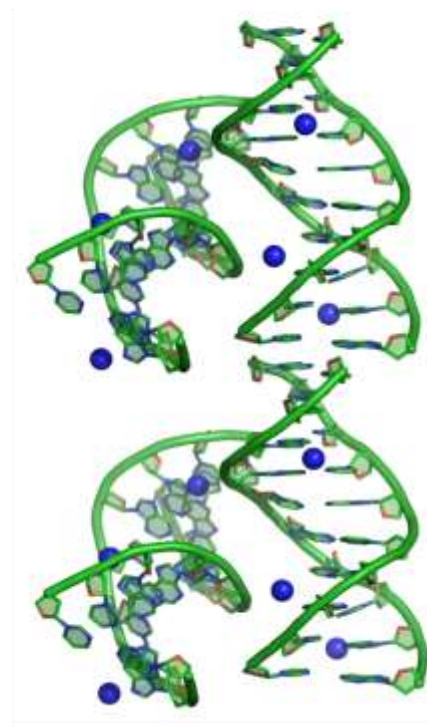
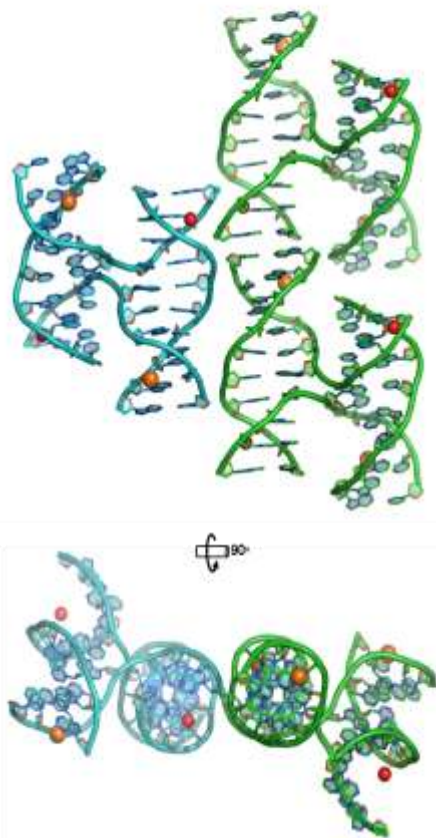


Figure S2: Comparison of crystal packing of racemic and non-racemic crystal structures of B-type duplexes formed from the sequence d(CCGGTACCGG) (bound by cobalt).

a) Racemic crystal structure of a B-type duplex formed from the sequence D/L-d(CCGGTACCGG). The crystal packing of this structure involves the formation of enantiopure pseudo-continuous helices (D-DNA coloured green, L-DNA coloured cyan). Pseudo-continuous helices of opposite handedness pack laterally, interlocking in a compact manner, with the nucleic acid backbones of one racemate slotting into the groove regions of neighboring DNA molecules of opposite chirality. All three of the B-type duplex racemic crystal structures reported in this work display this mode of crystal packing. b) Non-racemic crystal structure of a B-type duplex formed from the sequence D-d(CCGGTACCGG) (PDB ID 3R86 [Venkadesh *et al.*, 2012]). Pseudo-continuous helices are also present in the equivalent non-racemic crystal form of this B-type duplex structure, however, these pseudo-continuous helices are not able to interlock laterally as they do in racemic crystal form. Consequently, the packing of the non-racemic B-type duplex is less dense (see table S4), potentially explaining the significantly improved resolution of the racemic crystal form (1.49 Å) over the non-racemic crystal form (2.8 Å). D-DNA, green; L-DNA, cyan; cobalt ions, blue spheres.

a) Racemic structure of a four-way junction
Sequence: D/L d(CCGGTACCGG)
Space group: $C2/c$



b) Non-racemic structure of a four-way junction
Sequence: D d(CCGGTACCGG)
Space group: $C2$

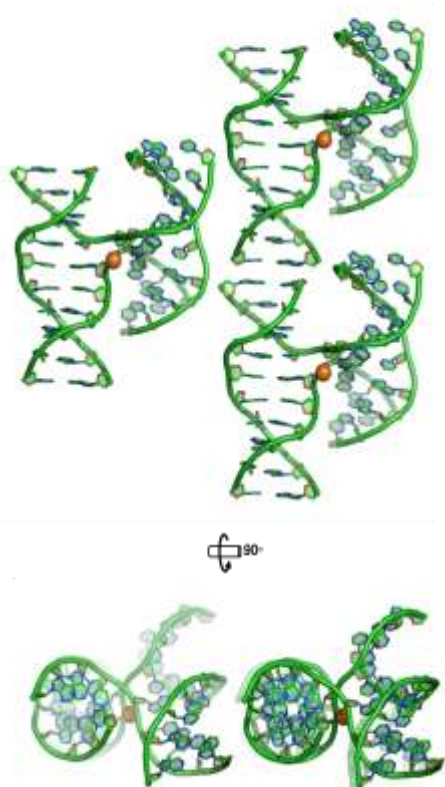
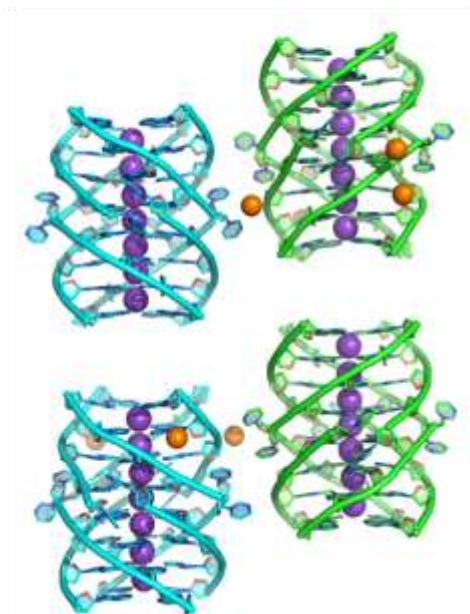


Figure S3: Comparison of crystal packing of racemic and non-racemic crystal structures of four-way DNA junctions formed from the sequence $d(\text{CCGGTACCGG})$.

a) Racemic crystal structure of a four-way junction formed from the sequence D/L - $d(\text{CCGGTACCGG})$. b) Equivalent non-racemic crystal structure of a four-way junction formed from the same sequence (PDB ID 1DCW [Eichman *et al.*, 2000]). The crystal packing of the racemic and non-racemic structures shown in (a) and (b) are surprisingly similar, despite the addition of achiral symmetry operators in the structure shown in (a). Crystal packing interactions include the formation of pseudo-continuous helices (comparable to those seen in Figure S2), as well as the lateral packing and interlocking of helices. D-DNA, green; L-DNA, cyan; sodium ions, orange spheres; calcium ions, red spheres.

a) Racemic structure of D/L d(TG₄T)
Space group: *P*-1



b) Non-racemic structure of D d(TG₄T)
Space group: *P*1

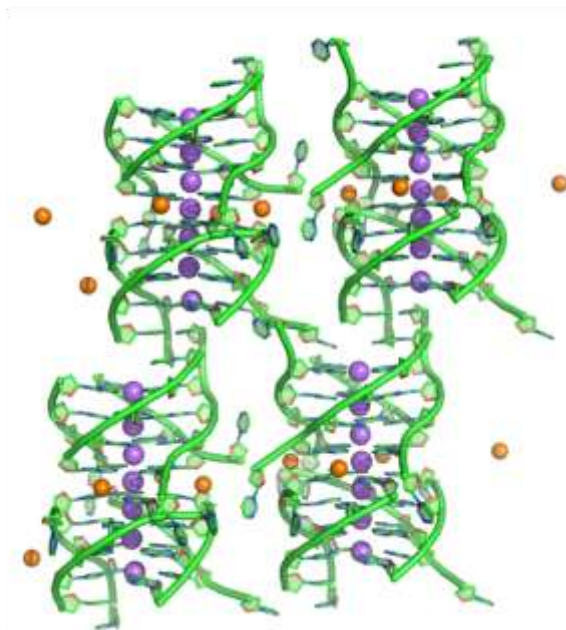


Figure S4: Comparison of crystal packing of racemic and non-racemic crystal structures of tetramolecular G-quadruplexes formed from the sequence d(TG₄T).

a) Crystal packing interactions of the racemic crystal form of the tetramolecular G-quadruplex formed from the sequence D/L-d(TG₄T) primarily involve the lateral ion-mediated packing of G-quadruplexes of opposite handedness. Additionally, G-quadruplexes of the same handedness pack longitudinally, aligning the centrally coordinated potassium ions of the G-quartets (magenta spheres). b) The equivalent non-racemic structure (PDB ID 352D [Philips *et al.*, 1997]) crystal packing also features the lateral packing of G-quadruplexes, however, the G-quadruplexes are not aligned longitudinally, instead, the coordinated potassium ions are offset relative to each G-quadruplex dimer. It is clear that there are more inter-quadruplex packing interactions present in the non-racemic structure compared to the racemic structure, which may explain the increased resolution of the non-racemic structure compared to the racemic form. D-DNA, green; L-DNA, cyan; potassium ions, magenta spheres; sodium ions, orange spheres.

3 Supplementary Tables

Table S1: Comparison of racemic and non-racemic DNA crystallogenesis.

DNA motif	Racemic			Non-Racemic			References
	Crystallization solution	Reservoir solution	Crystallogenesis (Temperature, duration and morphology)	Crystallization solution	Reservoir solution	Crystallogenesis (Temperature, duration and morphology)	
Tetramolecular G-Quadruplex	1 mM D/L-TG ₄ T ^[a] 100 mM MgCl ₂ ·6H ₂ O, 1.7 M 1,6-Hexanediol	200 mM MgCl ₂ ·6H ₂ O, 3.4 M 1,6-Hexanediol	293 K, 75 days, Rod-like crystals	1 mM D-TG ₄ T ^[b] 20 mM Sod. Cacodylate (pH 6.6), 12 mM CaCl ₂ , 130 - 180 mM NaCl, 6 mM Spermine tetrahydrochloride, 5% v/v MPD	120 mM Sod. Cacodylate (pH 6.6), 70 mM CaCl ₂ , 700 - 1M NaCl, 26-32 % v/v MPD	277-279 K, 14 days, Twinned crystals	Philips <i>et al.</i> , 1997
Bimolecular G-Quadruplex (Crystal form: I)	1 mM D/L-G ₄ T ₄ G ₄ ^[a] 50 mM MgCl ₂ ·6H ₂ O, 2.5 mM Spermine, 5% v/v MPD	35% v/v MPD	285 K, 90 days, Rod-like crystals	1 mM D- G ₄ T ₄ G ^[c] 40 mM KCl, 10 mM MgCl ₂ ·6H ₂ O, 4.1 mM Spermine 5% v/v MPD	35% v/v MPD	285 K, 14-28 days, Rod-like crystals	Haider <i>et al.</i> , 2002
Bimolecular G-Quadruplex (Crystal form: II)	1 mM D/L-G ₄ T ₄ G ₄ ^[a] 75 mM MgCl ₂ ·6H ₂ O, 2.5 mM Spermine, 5% v/v MPD	35% v/v MPD	285 K, 45 days, Rod-like crystals				
Four-way Junction	1 mM D/L-CCGGTACCGG, 75 mM Sod.Cacodylate (pH 7.0), 30 mM CaCl ₂ ·2H ₂ O, 1 mM Spermine	35% v/v MPD	293 K, 7 days, Bevelled diamonds	0.25 mM D-CCGGTACCGG, 75 mM Sod.Cacodylate (pH 7.0), 15 mM CaCl ₂ ·2H ₂ O, 2.5% v/v MPD	30% v/v MPD	293 K, Thin, diamond-shaped crystals	Eichman <i>et al.</i> , 2000
B-type duplex (Ca bound)	1 mM D/L-CCGGTACCGG, 50 mM Sod. Cacodylate (pH 7.0), 2 M CaCl ₂ ·2H ₂ O, 1 mM Spermine	40% v/v MPD	293 K, 14 days, Triclinic crystals	<i>Yet to be reported</i>	-	-	-
B-type duplex (Co bound)	0.5 mM D/L-CCGGTACCGG, 75 mM Sod. Cacodylate (pH 7.0), 10 mM CoCl ₂ ·6H ₂ O, 1 mM Spermine	40% v/v MPD	293 K, 7 days, Triclinic crystals	1 mM D-CCGGTACCGG, 50 mM Sod.Cacodylate (pH 7.0), 10 mM CoCl ₂ ·6H ₂ O, 1mM Spermine	50% v/v MPD	293 K, 7 days, Hexagonal prisms	Venkadesh <i>et al.</i> , 2012
B-type duplex (Mg bound)	1 mM D/L-CCGGTACCGG, 50 mM Sod. Cacodylate (pH 7.0), 200 mM MgCl ₂ ·6H ₂ O, 2.5 mM Spermine	30% v/v MPD	293 K, 30 days, Triclinic crystals	<i>Yet to be reported</i>	-	-	-

^[a] D/L-oligonucleotides annealed (in 50 mM potassium cacodylate buffer, pH 6.5 and 80 mM KCl) at 353 K for 20 minutes and gradually cooled to room temperature (RT) overnight.

^[b] D-TG₄T annealed (in 5 mM Hepes, pH 7.0 and 0.1 M NaCl) at 343 K for 20 min and gradually cooled to RT overnight

^[c] D-G₄T₄G₄ annealed (in potassium cacodylate buffer, pH 6.5) at 353 K for 15 min and gradually cooled to RT overnight

Abbreviations: MPD = 2-Methyl-2,4-pentanediol; PEG 400 = Polyethylene glycol 400.

Table S2: X-ray diffraction data and refinement statistics.

D/L-DNA (5'-3')	TG4T	G4T4G4		CCGGTACCGG			
		I	II	Ca	Ca	Co	Mg
Data collection							
X-ray source	FRX (<i>in-house</i>)	FRX (<i>in-house</i>)	FRX (<i>in-house</i>)	Proxima-1 (SOLEIL)	ID23-2 (ESRF)	Proxima-1 (SOLEIL)	Proxima-1 (SOLEIL)
Wavelength (Å)	1.5418	1.5418	1.5418	0.9998	0.873	0.9998	0.9998
Space group	<i>P</i> -1	<i>P</i> -1	<i>P</i> 2 ₁ / <i>n</i>	<i>C</i> 2/ <i>c</i>	<i>P</i> -1	<i>P</i> -1	<i>P</i> -1
Unit cell parameters (Å, °)	<i>a</i> = 39.94 <i>b</i> = 39.00 <i>c</i> = 84.08 α = 103.34 β = 103.37 γ = 90.04	<i>a</i> = 27.65 <i>b</i> = 28.30 <i>c</i> = 45.72 α = 104.50 β = 94.19 γ = 113.42	<i>a</i> = 28.50 <i>b</i> = 47.20 <i>c</i> = 46.80 α = 90.00 β = 97.02 γ = 90.00	<i>a</i> = 65.95 <i>b</i> = 23.35 <i>c</i> = 72.91 α = 90.00 β = 115.47 γ = 109.78	<i>a</i> = 23.26 <i>b</i> = 33.60 <i>c</i> = 36.82 α = 103.32 β = 101.02 γ = 109.78	<i>a</i> = 26.29 <i>b</i> = 32.35 <i>c</i> = 33.50 α = 62.25 β = 73.14 γ = 68.56	<i>a</i> = 31.61 <i>b</i> = 32.95 <i>c</i> = 46.25 α = 70.76 β = 80.77 γ = 73.77
Resolution (Å)	17.51- 2.69 (2.79-2.69)*	25.02 - 1.90 (1.97-1.90)	24.28 - 1.85 (1.91-1.85)	32.91 - 2.33 (2.41 - 2.33)	34.25 - 1.28 (1.32 - 1.28)	29.33 - 1.49 (1.54 - 1.49)	43.54 - 1.29 (1.37 - 1.29)
Total reflections	20816 (2054)	15065 (1335)	19372 (1989)	8312 (734)	46075 (4157)	25501 (3984)	74343 (11071)
Unique reflections	12597 (1292)	9011 (909)	9892 (1009)	4156 (367)	23975 (2314)	14025 (1339)	38749 (5913)
<i>R</i> _{merge}	0.1643 (0.4338)	0.0628 (0.1227)	0.0736 (0.1591)	0.0442 (0.2929)	0.0372 (0.2656)	0.0480 (0.1980)	0.0230 (0.303)
Mean <i>I</i> / σ (<i>I</i>)	1.7 (1.6)	7.81 (2.66)	10.25 (3.47)	4.55 (1.68)	9.69 (2.39)	10.81 (4.98)	14.11 (2.57)
Wilson B factor (Å ²)	49.77	49.29	49.16	49.84	47.43	48.09	47.68
Completeness (%)	97.69 (97.34)	94.89 (95.66)	93.60 (96.52)	99.33 (94.34)	95.23 (91.68)	95.38 (89.57)	91.40 (86.2)
Multiplicity	1.7 (1.6)	1.7 (1.5)	1.9 (1.9)	2.0 (2.0)	1.9 (1.8)	1.9 (1.9)	1.9 (1.9)
Cell content							
Matthews coefficient <i>V</i> _M (Å ³ Da ⁻¹)	2.02	2.06	2.07	2.09	2.09	1.92	1.80
No. of molecules in asymmetric unit	4 tetramolecular G-quadruplexes	1 bimolecular G-quadruplex	1 bimolecular G-quadruplex	1 crossing strand, 1 non-crossing strand	1 B-DNA duplex	1 B-DNA duplex	2 B-DNA duplex
Solvent content (%)	59	60	60	60	60	57	54
SEARCH MODEL (PDB ID) FOR MR	352D	2HBN	1JRN	1DCW	3R86	3R86	3R86
Refinement							
Resolution (Å)	37.89 - 2.70	25.02 - 1.90	24.28 - 1.85	32.91 - 2.33	34.25 - 1.28	29.33 - 1.49	43.54 - 1.29
<i>R</i> _{work} / <i>R</i> _{free}	0.2954/0.3253	0.2856/0.3400	0.2826/0.3036	0.2887/0.3409	0.2188/0.2596	0.2089/0.2326	0.2689/0.3113
No. of reflections	11917	8599	9376	4142	22744	13328	37851
No. of non-H atoms	1725	658	672	428	580	564	1111
DNA	1706	506	506	404	404	404	808
Ions/Ligands	14 K ⁺ , 4 Na ⁺	5 K ⁺	5 K ⁺ , 3 Mg ²⁺	1 Ca ²⁺ , 1 Na ⁺	7 Ca ²⁺ , 2 Na ⁺	1 Spermine, 5 Co ²⁺	8 Mg ²⁺ , 1 Na ⁺
Water	1	143	151	22	167	109	134
R.m.s.d., bond (Å)	0.007	0.009	0.009	0.010	0.014	0.012	0.014
R.m.s.d., angle (°)	1.41	1.22	1.52	1.07	1.92	1.90	2.36
Mean B factor (Å ²)	31.90	15.10	12.40	46.60	14.30	12.40	18.50
DNA	32.00	12.70	9.40	46.50	11.50	10.80	17.50
Ions	25.80	7.40	16.50	58.90	12.60	16.20	15.60
Water	51.30	23.50	21.80	46.70	21.30	18.40	25.90
PDB ID	4R44	4R45	4R47	4R48	4R49	4R4A	4R4D

*Values in parenthesis refer to highest resolution shell.

Table S3: Root mean square deviation (RMSD) values (in Å) of the reference D-DNA crystal structures superposed to D-DNA structures obtained from racemic crystallization.

	D-TG ₄ T* (4R44)	D-G ₄ T ₄ G ₄ (4R45)	D-G ₄ T ₄ G ₄ (4R47)	D-CCGGTACCGG (4R48)	D-CCGGTACCGG (4R49)	D-CCGGTACCGG (4R4A)	D-CCGGTACCGG (4R4D)		Reference
							Duplex 1	Duplex 2	
D-TG ₄ T (352D)*	0.56	-	-	-	-	-	-	-	Philips <i>et al.</i> , 1997
D-G ₄ T ₄ G ₄ (2HBN)	-	0.32	0.32	-	-	-	-	-	Gill <i>et al.</i> , 2006
D-G ₄ T ₄ G ₄ (1JRN)	-	0.35	0.31	-	-	-	-	-	Haider <i>et al.</i> , 2002
D-CCGGTACCGG (1DCW)	-	-	-	0.39	-	-	-	-	Eichman <i>et al.</i> , 2000
D-CCGGTACCGG (3R86)	-	-	-	-	1.44	1.45	1.45	1.38	Venkadesh <i>et al.</i> , 2012

Search models used for molecular replacement were used for RMSD calculations using *Superpose* (Krissinel and Henrick, 2004)

*TG₄T: all atom coordinates of the G-quartets alone used for least square superposition

Table S4: Comparison of resolution and solvent content of racemate with the reference D-DNA crystal structures

	PDB Entry	Maximal resolution	Space group	Solvent content
D/L-TG ₄ T (K ⁺)	4R44	2.69 Å	<i>P</i> -1	59 %
D-TG ₄ T	352D	0.95 Å	<i>P</i> 1	64 %
D/L-G ₄ T ₄ G ₄ (K ⁺) form-1	4R45	1.90 Å	<i>P</i> -1	60 %
D-G ₄ T ₄ G ₄	2HBN	1.55 Å	<i>P</i> 2 ₁ 2 ₁ 2 ₁	60 %
D/L-G ₄ T ₄ G ₄ (K ⁺) form-2	4R47	1.85 Å	<i>P</i> 2 ₁ /n	60 %
D-G ₄ T ₄ G ₄	1JRN	2.00 Å	<i>P</i> 2 ₁ 2 ₁ 2 ₁	58 %
D/L-CCGGTACCGG (Ca ²⁺)	4R48	2.33 Å	<i>C</i> 2/ <i>c</i>	60 %
D-CCGGTACCGG	1DCW	2.10 Å	<i>C</i> 2	63 %
D/L-CCGGTACCGG (Co ²⁺)	4R4A	1.49 Å	<i>P</i> -1	57 %
D-CCGGTACCGG	3R86	2.86 Å	<i>P</i> 6 ₁	65 %

References

- A. J. McCoy, R.W. Grosse-Kunstleve, P. D. Adams, M. D. Winn, L. C. Storoni, R. J. Read, *J. Appl. Crystallogr.* **2007**, *40*, 658–674.
- B. F. Eichman, J. M. Vargason, B. H. Mooers, P. S. Ho, *Proc. Natl. Acad. Sci. USA*, **2000**, *97*, 3971–3976.
- B. W. Matthews, *J. Mol. Biol.* **1968**, *33*, 491–497.
- C. Caceres, G. Wright, C. Gouyette, G. Parkinson, J. A. Subirana, *Nucleic Acids Res.* **2004**, *32*, 1097–1102.
- E. Krissinel and K. Henrick, *Acta Cryst.* **2004**, *D60*, 2256–2268.
- G. N. Murshudov, P. Skubák, A. A. Lebedev, N. S. Pannu, R. A. Steiner, R. A. Nicholls, M. D. Winn, F. Long, A. A. Vagin, *Acta Crystallogr., Sect. D* **2011**, *67*, 355–367.
- H. M. Berman, J. Westbrook, Z. Feng, G. Gilliland, T. N. Bhat, H. Weissig, I. N. Shindyalov, P. E. Bourne, *Nucleic Acids Res.* **2000**, *28*, 235–242.
- K. Phillips, Z. Dauter, A. I. Murchie, D. M. Lilley, B. Luisi, *J. Mol. Biol.* **1997**, *273*, 171–182.
- M. D. Winn, C. C. Ballard, K. D. Cowtan, E. J. Dodson, P. Emsley, P. R. Evans, R. M. Keegan, E. B. Krissinel, A. G. W. Leslie, A. McCoy, S. J. McNicholas, G. N. Murshudov, N. S. Pannu, E. A. Potterton, H. R. Powell, R. J. Read, A. A. Vagin, K. S. Wilson, *Acta Crystallogr., Sect. D* **2011**, *67*, 235–242.
- M. L. Gill, S. A. Strobel, J. P. Loria, *Nucleic Acids Res.* **2006**, *34*, 4506–4514.
- M. P. Lee, G. N. Parkinson, P. Hazel, S. Neidle, *J. Am. Chem. Soc.* **2007**, *129*, 10106–10107.
- P. D. Adams, P.V. Afonine, G. Bunkoczi, V. B. Chen, I. W. Davis, N. Echols, J. J. Headd, L. –W. hung, G. J. Kapral, R. W. Grosse-Kunstleve, A. J. McCoy, N. W. Moriarty, R. Oeffner, R. J. Read, D. C. Richardson, J. S. Richardson, T. C. Terwilliger, P. H. Zwart, *Acta Cryst. D* **2010**, *66*, 213–221.
- P. Emsley, B. Lohkamp, K. Cowtan, *Acta Crystallogr., Sect. D* **2010**, *66*, 486–501.
- P. Hazel, G. N. Parkinson, S. Neidle, *J. Am. Chem. Soc.* **2006**, *128*, 5480–5487.
- P. V. Afonine, R. W. Grosse-Kunstleve, N. Echols, J. J. Headd, N. W. Moriarty, M. Mustyakimov, T. C. Terwilliger, A. Urzhumtsev, P. H. Zwart, P. D. Adams, *Acta Crystallogr., Sect. D* **2012**, *68*, 352–367.
- S. Haider, G. N. Parkinson, S. Neidle, *J. Mol. Biol.* **2002**, *320*, 189–200.
- S. Venkadesh, P. K. Mandal, N. Gautham, *Nucleos. Nucleot. Nucl.* **2012**, *31*, 184–196.
- W. Kabsch, *Acta Crystallogr., Sect. D* **2010**, *66*, 125–132.
- W. L. DeLano, *The PyMOL Users Manual* **2002**, DeLano Scientific, San Carlos, California, USA.